JOURNAL OF AIRCRAFT
Vol. 38, No. 2, March–April 2001

Influence of Yaw Cards on the Yaw Growth of Spin-Stabilized Projectiles

G. R. Cooper*
U.S. Army Research Laboratory, Aberdeen Proving Ground, Maryland 21005-5066

A simple extension of the standard linear theory, describing the free-flight motion of a projectile, now includes the influences due to the projectile impacting yaw cards. The card impacts are modeled as ideal delta function impulses that are shown to alter the usual yawing motion of a spin-stabilized projectile passing through a yaw card range. Card-induced changes in the complex-valued yaw modes are expressed as difference equations. Known analytic solutions to these difference equations show how card impacts influence a projectile's yawing motion by relating simple expressions of the card spacing to a parameter describing the material density of the yaw cards. These solutions also reveal that both bounded and unbounded yaw mode magnitudes can be induced by yaw card impacts. Furthermore, the model shows that moments caused by repeated projectile and card interactions should not always be treated as negligible. Examples of these results for a typical small arms projectile (7.62 mm) launched from an unworn gun tube are presented.

Nomenclature

A	=	reference area, $\pi d^2/4$
C_{M_α}	=	aerodynamic moment overturning coefficient
$C_{M_{\alpha c}}$	=	overturning moment coefficient for card material
d	=	projectile reference diameter
d_c	=	nondimensional card spacing when cards are uniformly spaced
g	=	card stability constant, $\mu \sin(\gamma/2) + \cos(\gamma/2)$
I_c	=	nondimensional card overturning impulse, $(\rho_c A d^2 \tau_c C_{M\alpha})/(2I_y)$
I_x	=	axial moment of inertia
I_y	=	transverse moment of inertia
i	=	$\sqrt{-1}$
j	=	card index value, 0, 1, 2, ...
$\bar{K}_{m,j}$	=	average mode magnitude
$K_{1,j}$	=	fast yaw mode magnitude before transiting the jth card
$K_{2,j}$	=	slow yaw mode magnitude before transiting the jth card
M	=	nondimensionalized overturning moment, $(\rho A d^3 C_{M\alpha})/(2I_y)$
M_c	=	nondimensionalized card overturning moment, $(\rho_c A d^3 C_{M\alpha_c})/(2I_y)$
m	=	mode number, 1 or 2
$\dot{m}$	=	projectile mass
N	=	maximum number of cards
P	=	$(I_x p d)/(I_y V)$
p	=	axial spin rate
q	=	real number
S_g	=	gyroscopic stability factor
S_{j+1}	=	phase value for jth + 1 card, $(\phi_1' - \phi_2')s_j$
s	=	nondimensional trajectory arc length (calibers), that is, Vt/d
s_j	=	s at jth card
t	=	time
V	=	magnitude of velocity
Z	=	set of integers
Z^e	=	set of even integers
Z^o	=	set of odd integers
α	=	angle of attack
β	=	angle of sideslip
$[\alpha, \beta]_\mp$	=	$\alpha\beta^* \mp \alpha^*\beta$ commutator and anticommutator
γ	=	phase interval between uniformly spaced cards, $S_{j+1} - S_j$
ΔK	=	modal magnitude change
$\Delta\phi$	=	epicyclical phase jump
$\kappa_{1,j}$	=	complex amplitude of fast mode, $K_{1,j}\exp(i\phi_{1,j})$
$\kappa_{2,j}$	=	complex amplitude of slow mode, $K_{2,j}\exp(i\phi_{2,j})$
μ	=	impact stability parameter, $I_c/(\phi_1' - \phi_2')_1$
ξ	=	complex yaw, $\sin\beta + i\sin\alpha$
ρ	=	air density
ρ_c	=	card material density
τ_c	=	card thickness
Φ_{j+1}	=	phase encounter angle
$\hat{\phi}_j$	=	$(\phi_{1,j} - \phi_{2,j})$
$\phi_{1,j}$	=	fast mode phase angle, between $j-1$ and jth card
$\phi_{2,j}$	=	slow mode phase angle, between $j-1$ and jth card
ϕ_1'	=	fast mode angular rate
ϕ_2'	=	slow mode angular rate
$'$	=	d( )/ds
*	=	complex conjugate
||	=	absolute value $\|x + iy\| = \sqrt{(x^2 + y^2)}$

Received 29 March 1999; revision received 20 July 2000; accepted for publication 4 November 2000. This material is declared a work of the U.S. Government and is not subject to copyright protection in the United States.

*Research Physicist, Aerodynamic Branch. Senior Member AIAA.

Introduction

YAW card arrays placed in a firing range have been used to obtain flight data when spark ranges are not available or when spark range operations are possibly compromised. A projectile impacting a yaw card produces an elongated hole depicting the silhouette of this projectile normal to the line of fire. Comparing the dimensions of this hole to the dimensions of the projectile plus measuring the hole orientation, relative to some fixed axis, enables one to determine the pitch and yaw angles of this projectile at that card's location. The interactions of the projectile with yaw cards cause the reduced flight coefficients to differ from the values found from nonintrusive photographic measurements taken in a spark range. McCoy[1] addressed this problem using Fourier analysis along with an averaging procedure to account for these discrepancies. His conclusion was that the small perturbations generated by yaw card interactions gave an additional average phase shift to the usual projectile yawing motion. The projectile flight data were then corrected to account for this phase shift.

Cooper and Fansler[2] modeled the projectile and card interaction using Dirac delta functions. This approach eliminated the averaging technique. They calculated the fast and slow mode changes in magnitude, as well as the corresponding phase changes at each card. Because the materials used in manufacturing yaw cards are dense when

compared to air density, it is reasonable to expect that sufficiently decreasing yaw card spacing or using thick yaw cards might result in projectile destabilization. In particular, marginally stable projectiles would require careful design of the range to avoid inducing instability. McCoy[1] asserted that the usual stability criterion, extended with his correction due to yaw cards, was still valid. Cooper and Fansler[2] validated this assertion, provided that a stability parameter arising from yaw card interaction is assumed small.

The current approach is an analytical continuation of the computer simulations given by Cooper and Fansler.[2] As before, interactions of the projectile with yaw cards are treated as ideal impulses. However, in the present study, both uniform and nonuniform card spacing are examined. This approach produces first- and second-order difference equations with known solutions. These closed-form solutions yield an additional stability criterion for projectiles flying through a uniformly spaced yaw card range. Both stable and unstable yaw modes are examined, and closed-form expressions for modal magnitudes, plus the corresponding phase angles, are given as functions of the number of yaw cards. These analytical results also explain the computer simulated results given previously.[2]

Governing Equation of Motion

The differential equation of pitching and yawing motion for a spinning projectile, acted on by a linear pitching moment and with damping processes neglected, is, in Murphy's[3] notation,

$$\xi'' - iP\xi' - M\xi = 0 \tag{1}$$

Solutions to Eq. (1) are written according to Murphy[3] as epicyclic motion

$$\zeta = K_1 \exp(i\phi_1 + i\phi_1' s) + K_2 \exp(i\phi_2 + i\phi_2' s)$$

$$\phi_m' = \left(P \pm \sqrt{P^2 - 4M}\right)/2, \qquad m = 1,\ 2$$

where K_1 and K_2 are magnitudes of the two modes with initial phases ϕ_1 and ϕ_2 having angular rates ϕ_1' and ϕ_2'. Because Eq. (1) is the equation of motion of a projectile flying through air, modifications must be introduced to account for the denser yaw cards. Following Cooper and Fansler,[2] a nondimensional card-overturning moment M_c along with the corresponding impulse I_c are defined as

$$M_C = \left(\rho_c A d^3/2I_y\right) C_{Mac}, \qquad I_c = \left(\rho_c A d^2 \tau_c/2I_y\right) C_{Mac} \tag{2}$$

for the card material density ρ_c.

Equation (1) will now be modified to account for the yaw card interactions. We will assume that each yaw card transmits an overturning moment to the projectile. This moment is modeled as an ideal Dirac delta function impulse, $\delta(s - s_j)$, located at the jth card with position s_j. Using the pitching moment impulse I_c, we replace M with

$$M + I_c \sum_{j=1}^{n} \delta(s - s_j)$$

changing the governing Eq. (1) to

$$\xi'' - iP\xi' - \left[M + I_c \sum_{j=1}^{n} \delta(s - s_j)\right]\xi = 0 \tag{3}$$

The modal solution of Eq. (3) between the jth and jth $+ 1$ cards can be written by extending Murphy's notation[3]

$$\zeta = K_{1,j} \exp(i\phi_{1,j} + i\phi_1' s) + K_{2,j} \exp(i\phi_{2,j} + i\phi_2' s)$$

$$j = 0,\ 1,\ \ldots,\ N$$

$$\phi_m' = \left(P \pm \sqrt{P^2 - 4M}\right)/2, \qquad m = 1,\ 2 \tag{4}$$

where $K_{1,j}$ and $K_{2,j}$ are the card-modified fast and slow modal magnitudes having $\phi_{1,j}$ and $\phi_{2,j}$ as card-modified fast and slow initial phase angles. The respective phase angular rates ϕ_1' and ϕ_2' are unchanged by the projectile and card interaction. Note that $j = 0$ means that the projectile has not reached the first yaw card and that Eqs. (4) describe the usual epicycloid motion associated with free-flight projectiles moving between adjacent cards.

For convenience, the modes are written in polar form as

$$\kappa_{m,j} = K_{m,j} e^{i\phi_{m,j}}, \qquad m = 1,\ 2, \qquad j = 0,\ 1,\ 2,\ \ldots,\ N \tag{5}$$

transforming the first equation in Eqs. (4) to

$$\xi = \kappa_{1,j} e^{i\phi_1' s} + \kappa_{2,j} e^{i\phi_2' s} \tag{6}$$

Boundary conditions at each card for Eq. (3) are given by

$$\xi(s_{j+}) = \xi(s_j), \qquad \xi'(s_{j+}) - \xi'(s_j) = I_c \xi(s_j) \tag{7}$$

that show the usual discontinuous derivative caused by delta functions.

Modal Parameters Before and After a Single Card Interaction

Here we will examine single card impacts that may or may not require uniform yaw card spacing. The following section will take up the discussion where the cards are constrained to uniform spacing. Consider a projectile impacting the jth $+ 1$ card. Substituting Eq. (6) into Eqs. (7), then solving for $\kappa_{1,j+1}$ and $\kappa_{2,j+1}$ in terms of $\kappa_{1,j}$ and $\kappa_{2,j}$, results in a coupled system of difference equations for the complex valued $\kappa_{1,j}$ and $\kappa_{2,j}$

$$\kappa_{1,j+1} = \kappa_{1,j} - i\mu\kappa_{1,j} - i\mu\kappa_{2,j} e^{-iS_{j+1}}$$

$$\kappa_{2,j+1} = \kappa_{2,j} + i\mu\kappa_{2,j} + i\mu\kappa_{1,j} e^{iS_{j+1}} \tag{8}$$

Defining the parameters μ and S_j as[2]

$$\mu = I_c/(\phi_1' - \phi_2') = I_c/\sqrt{P^2 - 4M}$$

$$S_j = (\phi_1' - \phi_2')s_j = \sqrt{P^2 - 4M}\, s_j \tag{9}$$

and manipulating Eqs. (8), using the usual trigonometric reduction formulas, shows that the modal magnitudes before and after a card impact are related as

$$\left|\frac{K_{m,j+1}}{K_{m,j}}\right|^2 - 1 = -2\mu \frac{K_{3-m,j}}{K_{m,j}} \sin(\Phi_{j+1}) + \mu^2 \left[1 + \left(\frac{K_{3-m,j}}{K_{m,j}}\right)^2 + 2\frac{K_{3-m,j}}{K_{m,j}} \cos(\Phi_{j+1})\right], \qquad m = 1,\ 2$$

$$\Phi_{j+1} = S_{j+1} + \hat{\phi}_j, \qquad \hat{\phi}_j = \phi_{1,j} - \phi_{2,j} \tag{10}$$

Here we introduce the angle Φ_{j+1}, which is called the phase encounter angle at the jth $+ 1$ yaw card. Applying $[\kappa_{m,j+1}, \kappa_{m,j}]_-/[\kappa_{m,j+1}, \kappa_{m,j}]_+$ to Eqs. (8), rewritten in polar form, yields an expression for the changes in the modal phase angles $\phi_{m,j+1} - \phi_{m,j}$, $m = 1,\ 2$, caused by the projectile impacting the jth $+ 1$ card:

$$\tan(\phi_{m,j+1} - \phi_{m,j}) = (-1)^{m+1} \frac{[K_{3-m,j} \cos(\Phi_{j+1}) + K_{m,j}]\mu}{K_{3-m,j} \sin(\Phi_{j+1})\mu - K_{m,j}}$$

$$m = 1,\ 2 \tag{11}$$

Subtracting the two modal equations found in Eqs. (10) leads to an invariant relation for the two modes:

$$K_{1,j+1}^2 - K_{2,j+1}^2 = K_{1,j}^2 - K_{2,j}^2$$

or

$$K_{1,j}^2 - K_{2,j}^2 = K_{1,0}^2 - K_{2,0}^2$$

showing that the modal magnitudes lie along a hyperbola.

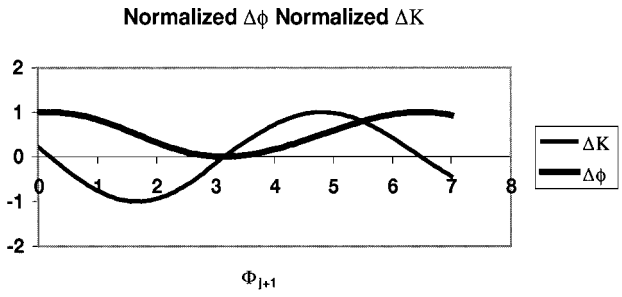

Fig. 1 Normalized phase change and normalized modal magnitude.

We define the epicyclical phase jump $\Delta\phi$ and the modal magnitude change ΔK, attributable to a single impact at the jth + 1 card, as

$$\Delta\phi = \phi_{m,j+1} - \phi_{m,j}, \qquad \Delta K = |K_{m,j+1}/K_{m,j}| - 1$$
$$\text{for} \quad m = 1,\ 2, \qquad j = 0,\ 1,\ 2, \ldots, N \tag{12}$$

Whenever $K_{1,j} = K_{2,j}$, Eq. (11) tells us that $\phi_{1,j+1} - \phi_{1,j} + \phi_{2,j+1} - \phi_{2,j} = n\pi$, $n \in Z$. Because μ is usually small, physical arguments demand that $\phi_{m,j+1} - \phi_{m,j} \to 0$ as $\mu \to 0$ for both $m = 1,\ 2$. We, therefore, see that the changes in the two modal phase angles are centered about $n\pi$, so that $\phi_{1,j+1} - \phi_{1,j} \to -(\phi_{2,j+1} - \phi_{2,j}) + n\pi$. Experience has shown that most often $n = 0$, which means that the two modes are rotated equally but in opposite directions. Figure 1 shows $\Delta\phi$ and ΔK, each normalized by their respective peak values, for a case wherein the two modal magnitudes are equal

$$\frac{\Delta\phi}{\Delta\phi_{\text{peak}}} = \frac{\tan^{-1}\{[\mu\cos(\Phi_{j+1}) + \mu]/[\mu\sin(\Phi_{j+1}) - 1]\}}{\tan^{-1}[2\mu/(\mu^2 - 1)]}$$

$$\frac{\Delta K}{\Delta K_{\text{peak}}} = \frac{\mu - \sqrt{\mu^2 + 1}\,\sin\left[\Phi_{j+1} - \tan^{-1}(\mu)\right]}{\left[\mu\,\text{signum}(\Phi_{j+1} - \pi) + \sqrt{\mu^2 + 1}\right]}$$

as functions of Φ_{j+1}.

Using the first equation of Eqs. (10), we now find the extreme values for maximum growth and maximum decay for the cases where the gun bore is assumed to be unworn, that is, the modes have equal magnitudes. Straightforward analysis tells us that $\cos[\Phi_{j+1} - \tan^{-1}(\mu)] = 0$. Now, solving for the phase encounter angle Φ_{j+1}, we find that $\Phi_{j+1} = \tan^{-1}(\mu) \pm (n\pi)/2$, $n \in Z^o$. Substituting this value of Φ_{j+1} back into the first of Eqs. (10), for both $m = 1, 2$, followed by some simplification, gives us

$$(K_{m,j+1}/K_{m,j})^2 - 1 = \pm 2\mu\sqrt{\mu^2 + 1} + 2\mu^2 \qquad \text{for} \qquad K_{1,0} = K_{2,0}$$

This last expression is a first-order linear difference equation that is easily solved $\{K_{m,j} = [\mu \pm \sqrt{(\mu^2 + 1)}]^j K_{m,0}\}$ to produce the maximum growth and decay rates shown in Fig. 2. The corresponding phase changes come from Eq. (11) and reveal that $\tan(\phi_{m,j+1} - \phi_{m,j}) = (-1)^m\mu$ for $m = 1, 2$. This can be solved for $\phi_{m,j+1}$ so that one will find that $\hat{\phi}_j = \hat{\phi}_0 + j\{\tan^{-1}[2\mu/(\mu^2 - 1)] + \hat{n}\pi\}$, $\hat{n} \in Z$. Because we already have the corresponding values of Φ_{j+1}, we can use the second equation of Eqs. (10) to find the needed card phase value S_{j+1} $j = 0, 1, 2, \ldots$ by remembering that S_1 is the phase value of the first yaw card. Notice that if n and $\hat{n}$ are constant, then the card spacing is uniform.

A similar analysis for both modes equal in magnitude so that $\Delta K = 0$ leads to $\sin[\Phi_{j+1} - \tan^{-1}(\mu)] = \mu/\sqrt{(\mu^2 + 1)}$. Now, solving for Φ_{j+1}, we find that

$$\Phi_{j+1} = -2\,\cot^{-1}(\mu) \pm \pi n, \qquad m = 1, 2, \qquad n \in Z^o$$

Placing this result into Eq. (11) tells us that

$$\hat{\phi}_j = \hat{\phi}_0 + j\{\tan^{-1}[4\mu(\mu^2 - 1)/(\mu^4 - 6\mu^2 + 1)] + \hat{n}\pi\}, \qquad \hat{n} \in Z$$

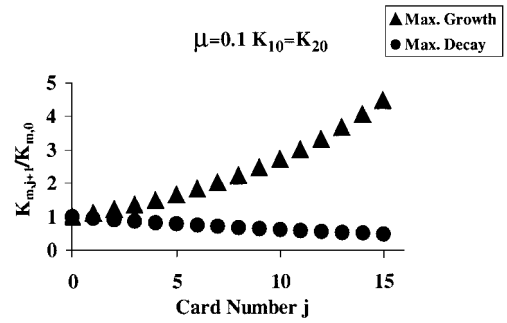

Fig. 2 Growth and decay of $K_{m,j}/K_{m,0}$ as functions of card number.

As before, we can find the card spacing S_{j+1} $j = 0, 1, 2, \ldots$, and, once again, if n and $\hat{n}$ are constant, then the card spacing is uniform. For completion, also note that $\Delta K = 0$ whenever $\Phi_{j+1} = n\pi$, $n \in Z^o$, implying that $\phi_{m,j+1} - \phi_{m,j} = n\pi$, $n \in Z$ for any value of μ when $m = 1, 2$ and $j = 0, 1, 2, \ldots$.

Difference Equations for Uniform Yaw Card Spacing

Yaw card ranges usually comprise a series of equally spaced cards to facilitate extraction of the projectile's flight coefficients. For this situation, we rewrite the coupled Eqs. (8) as uncoupled second-order difference equations:

$$\kappa_{1,j+2} - 2ge^{-i\gamma/2}\kappa_{1,j+1} + e^{-i\gamma}\kappa_{1,j} = 0$$
$$\kappa_{2,j+2} - 2ge^{i\gamma/2}\kappa_{2,j+1} + e^{i\gamma}\kappa_{2,j} = 0$$
$$\gamma = S_{j+1} - S_j$$
$$g = \mu\sin(\gamma/2) + \cos(\gamma/2) \tag{13}$$

Introducing $\kappa_{m,j} = Q_{m,j}(e^{i(-1)^m\gamma/2})^j$, $m = 1,\ 2$ and $j = 0,\ 1,\ 2, \ldots, N$ transforms Eqs. (13) to

$$Q_{m,j+2} - 2g\,Q_{m,j+1} + Q_{m,j} = 0, \qquad m = 1,\ 2 \tag{14}$$

in which g is defined as

$$g = \cos(\theta) \qquad \text{for} \qquad |g| < 1$$
$$g = \cosh(\theta) \qquad \text{for} \qquad g \geq 1$$
$$g = -\cosh(\theta) \qquad \text{for} \qquad g \leq -1 \tag{15}$$

Using the identities

$$\cos[\theta(q+2)] = 2\cos(\theta)\cos[\theta(q+1)] - \cos(q\theta)$$
$$\sin[\theta(q+2)] = 2\cos(\theta)\sin[\theta(q+1)] - \sin(q\theta)$$

for any real q, one can find solutions to Eq. (14) for $|g| \leq 1$. Including the initial conditions $\kappa_{m,0}$ and $\kappa_{m,1} = \kappa_{m,0}[(-1)^m i\mu + 1] + (-1)^m i\kappa_{3-m,0}$ for $m = 1,\ 2$, the two complex-valued modal amplitudes described by Eqs. (13) are readily obtained

$$\kappa_{1,j} = \frac{\exp[-i\gamma(j-1)/2]}{\sin(\theta)}\Big\{\left[\kappa_{1,0}(1 - i\mu) - i\mu\kappa_{2,0}e^{-iS_1}\right]\sin(j\theta)$$
$$- \kappa_{1,0}e^{-i\gamma/2}\sin[(j-1)\theta]\Big\}$$
$$\kappa_{2,j} = \frac{\exp[i\gamma(j-1)/2]}{\sin(\theta)}\Big\{\left[\kappa_{2,0}(1 + i\mu) + i\mu\kappa_{1,0}e^{iS_1}\right]\sin(j\theta)$$
$$- \kappa_{2,0}e^{i\gamma/2}\sin[(j-1)\theta]\Big\} \tag{16}$$

The corresponding solutions for $g \geq 1$ can be obtained by $\theta \to i\theta$ in Eqs. (16). Solutions for $g \leq -1$ are found by multiplying the right-hand sides of Eqs. (16) by $(-1)^j$ and then replacing $\sin(j\theta)$ with

$-\sin(j\theta)$ followed by $\theta \to i\theta$. Manipulating Eqs. (16) for the two modal magnitudes, one will get

$$\left(\frac{K_{m,j}}{K_{m,0}}\right)^2 - 1 = \frac{\sin(j\theta)\sin[(j+1)\theta]c_m + \sin^2(j\theta)d_m + \sin^2[(j-1)\theta] - \sin^2(\theta)}{\sin^2(\theta)}$$

$$c_m = 2\left[\frac{K_{3-m,0}}{K_{m,0}}\mu\sin(\gamma/2 - \Phi_1) + \cos(\theta)\right]$$

$$d_m = -\left[\frac{2K_{3-m,0}}{K_{m,0}}\mu[\sin(\Phi_1) - \mu\cos(\Phi_1)] - \frac{K_{3-m,0}^2}{K_{m,0}^2}\mu^2 - (\mu^2+1)\right] \tag{17}$$

where $m = 1$ or 2, $j = 0, 1, 2, \ldots, N$ and $\Phi_1 = S_1 + \phi_{1,0} - \phi_{2,0}$.

Equivalently, the modal magnitudes when $g \geq 1$ yields

$$\left(\frac{K_{m,j}}{K_{m,0}}\right)^2 - 1 = \frac{\sinh(j\theta)\sinh[(j+1)\theta]c_m + \sinh^2(j\theta)d_m + \sinh^2[(j-1)\theta] - \sinh^2(\theta)}{\sinh^2(\theta)}$$

$$c_m = 2\left[\frac{K_{3-m,0}}{K_{m,0}}\mu\sin(\gamma/2 - \Phi_1) + \cosh(\theta)\right]$$

$$d_m = -\left[\frac{2K_{3-m,0}}{K_{m,0}}\mu[\sin(\Phi_1) - \mu\cos(\Phi_1)] - \frac{K_{3-m,0}^2}{K_{m,0}^2}\mu^2 - (\mu^2+1)\right]$$

$$m = 1, 2, \qquad j = 0, 1, 2, \ldots, N, \qquad \Phi_1 = S_1 + \phi_{1,0} - \phi_{2,0} \tag{18}$$

and, for $g < -1$, we must replace $\cosh(\theta)$ with $-\cosh(\theta)$ and $\sinh(j\theta)$ with $-\sinh(j\theta)$ in Eqs. (18). One can see that when $|g| \geq 1$, Eqs. (18) will generally produce unbounded growing solutions. However, we will see in the next section that $|g| \geq 1$ does not always produce unbounded yawing motion. Whenever $|g| < 1$ is stable and bounded, yawing motion occurs. Cooper and Fansler[2] observed that the magnitudes of these modes lay in an envelope with midpoint averages generally not equal to zero. This can be explained by averaging Eqs. (17) over N yaw cards, and we will find that

$$\overline{\left|\frac{K_{m,j}}{K_{m,0}}\right|^2} - 1 = \frac{-1}{4N\sin^3(\theta)} \times \begin{bmatrix} c_m[\sin(2N\theta) - N\sin(2\theta)] \\ + d_m\{\sin[(2N+1)\theta] - (2N+1)\sin(\theta)\} \\ + \sin[(2N-1)\theta] + \sin(3\theta) - 2(N+1)\sin(\theta) \\ + 4(N+1)\sin^3(\theta) \end{bmatrix} \tag{19}$$

In the limiting case for large N, the right-hand side of Eq. (19) becomes $[d_m + 1 + c_m\cos(\theta) - 2\sin^2(\theta)]/[2\sin^2(\theta)]$. As γ varies so that the stability boundary is approached, that is, as $\theta \to 0$, this average diverges. Equations (16–19) indicate that ignoring the moments induced on a projectile when colliding with yaw cards may cause noticeable errors in the data reduction procedures used in extracting flight coefficients.

Yaw Growth ($|g| \geq 1$)

Whenever $|g| \geq 1$, the angle γ that determines the magnitude of $g = \mu\sin(\gamma/2) + \cos(\gamma/2)$ must satisfy

$$2n\pi \leq \gamma \leq 2n\pi + 4\tan^{-1}(\mu)$$

$$n \in Z^e \quad \text{for} \quad g \geq 1$$

$$n \in Z^o \quad \text{for} \quad g \leq -1$$

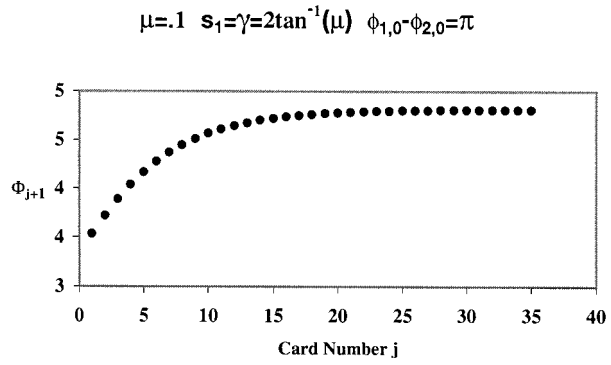

Fig. 3 Phase encounter value vs card index number.

Unless specified differently, we will let $n = 0$ for $g \geq 1$ and $n = 1$ for $g \leq -1$ because the general $|g| \geq 1$ requires simply adding an integer multiple of 4π to these values of γ. The usual approximate launch condition for an unworn gun, that is, $K_{1,0} = K_{2,0}$, will also be assumed. If we further assume that $\mu \ll 1$, then the second equation of Eqs. (15) shows that the usual gyroscopic stability factor S_g, given by Murphy,[3] can be written, with aid from Eqs. (2), as $S_g = P^2/4(M + M_c\tau_c/d_c) \leq 1$ for an unstable projectile. McCoy,[1] whose analysis is based on an approximation using an averaging method, also found this condition was true, but makes no reference to the size of μ.

Substituting $\theta \to i\theta$ into Eqs. (16) and letting j become large give the limiting equation

$$\kappa_{m,j+1} = \kappa_{m,j}\exp\{[(-1)^m i\gamma/2] + \theta\}, \qquad m = 1, 2 \tag{20}$$

Equation (20) says that the epicyclical phase jump $\Delta\phi$ approaches the phase interval $(-1)^m\gamma/2$ when j becomes large and we now have $\lim(\hat{\phi}_{j+1} - \hat{\phi}_j) \to -\gamma + n\pi$, $n \in Z$. Placing this limit into the second equation of Eqs. (10) tells us that $\lim(\Phi_{j+1})$ approaches a constant whenever the cards are spaced uniformly. Figure 3 shows an example of this limiting value as a function of the yaw card number j.

The next consideration is a case where the mode magnitudes decrease exponentially for sufficiently large j. One example of this is to take $0 \leq \gamma/2 \leq \tan^{-1}(\mu)$, which makes $g \geq 1$. Then, setting the coefficient of $e^{2j\theta}$ in Eq. (18) equal to zero, that is,

$$e^{-\theta}\sin(\gamma/2 - \Phi_1) + \sin(\Phi_1) - \mu\cos(\Phi_1) - \mu = 0$$

and then solving for Φ_1 gives

$$\tan\left(\frac{\Phi_1}{2}\right) = \frac{g\mu - \sqrt{\mu^2 - g^2 + 1}}{\sqrt{g^2 - 1}} + \mu \tag{21}$$

Rewriting this expression in terms of g, followed by some straightforward but lengthy algebra, we finally arrive at

$$K_{m,j}^2 = K_{m,0}^2\left(g - \sqrt{g^2-1}\right)^{2j}$$

$$m = 1,\ 2, \qquad j = 0,\ 1,\ 2, \ldots, N \tag{22}$$

One can see from the last equation that the modal magnitudes remain bounded even though $g \geq 1$. Substituting the preceding values of Φ_1 into Eq. (11), rewritten for equal mode magnitudes, and simplifying reveal

$$\tan(\phi_{1,1} - \phi_{1,0}) = -\left(g\sqrt{\mu^2 - g^2 + 1} - \mu\right)\Big/(\mu^2 - g^2)$$

$$\tan(\phi_{2,1} - \phi_{2,0}) = -\tan(\phi_{1,1} - \phi_{1,0}) \tag{23}$$

Now, solving Eqs. (23) for $\phi_{1,1}$ and $\phi_{2,1}$ allows us to calculate Φ_2, which, when placed into Eq. (11), gives $\phi_{1,2}$ and $\phi_{2,2}$. This procedure can be repeated for consecutive values of j so that $\phi_{1,j}$ and $\phi_{2,j}$ $j = 3,\ 4,\ 5, \ldots, N$ can be calculated. Alternatively, if we consider setting the coefficient of $e^{-j\theta}$ equal to zero, we will find exponentially growing solutions given by

$$\tan\left(\frac{\Phi_1}{2}\right) = \frac{\sqrt{\mu^2 - g^2 + 1} + g\mu}{\sqrt{g^2 - 1}} + \mu$$

$$K_{m,j}^2 = K_{m,0}^2\left(g + \sqrt{g^2 - 1}\right)^{2j}$$

$$m = 1,\ 2, \qquad j = 0,\ 1,\ 2, \ldots, N$$

with Eq. (23) remaining unchanged. One can see that similar calculations are feasible for any $\gamma/2$ that causes $|g| \geq 1$.

Further Illustrations

An example illustrating predicted results for the 7.62-mm projectile discussed previously by McCoy[1] and Cooper and Fansler[2] is examined. Shown in Fig. 4 is a parametric plot of α and β, where the nondimensional distance s is used as the parameter. For clarity, the effects of having no yaw card influence, $\mu = 0$, are compared to a typical sequence of six evenly spaced cards in which $\mu = 0.1$.

The fast and the slow modes initially have equal magnitudes, approximating the initial conditions for many projectiles. When starting at the origin, the curves coincide for the first phase distance S_1.

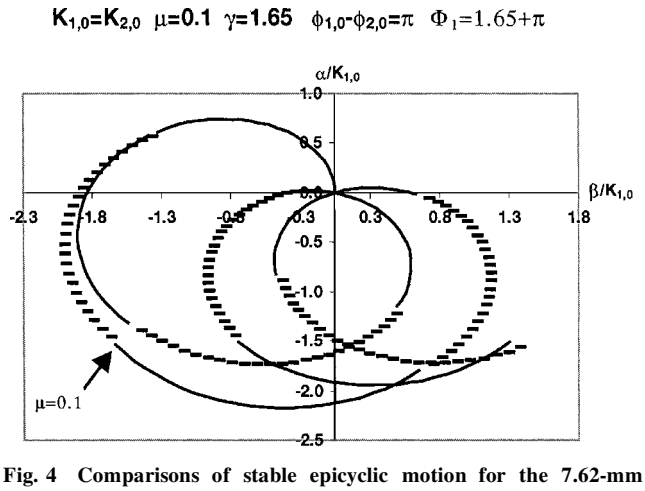

Fig. 4 Comparisons of stable epicyclic motion for the 7.62-mm projectile.

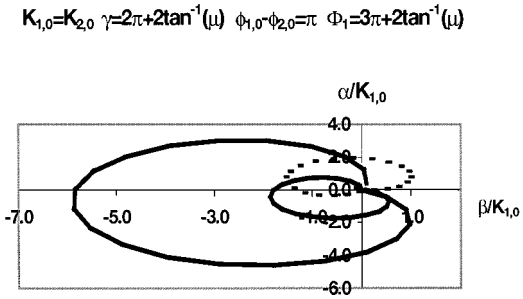

Fig. 5 Unstable epiclic motion for a 7.62-mm projectile.

This makes $\Phi_1 = 1.65 + \pi$, where one can see a discontinuity in the derivatives of α and β caused by the projectile's interaction with the first yaw card. Similar discontinuities occur for each of the following yaw cards, accounting for the discrepancies between the two parametric curves. After each impact, the curves alternate between dashed and solid lines to help distinguish yaw card positions.

Figure 5 shows the unstable epicyclical motion when the spacing between adjacent cards is such that the value of g is a maximum, that is, when $g = \sqrt{(1 + \mu^2)}$. This parametric plot also has alternate dashed and solid curves that indicate where the projectile and card impacts occur. Because $g \geq 1$, we see the modal magnitudes increase after each impact. In this example, the starting conditions are $\hat{\phi}_0 = \pi$ and the first card is positioned at $\Phi_1 = 3\pi + 2\tan^{-1}(\mu)$. Again, we have assumed unworn bore conditions so that $K_{1,0} = K_{2,0}$. As pointed out before, ignoring the moments caused by the yaw cards may result in nonnegligible errors. Figure 5 could falsely indicate an increasing yaw magnitude due to aerodynamic forces if the projectile and card collisions are ignored.

Conclusions

The disturbances imparted to the yawing motion of a free-flight projectile caused by collisions with yaw cards have been shown, at least in some cases, to be nonnegligible. Extending the linear theory of Murphy[3] to include projectile and card impacts results in simple expressions describing these disturbances. Considering a single card impact, under the assumption that the mode magnitudes are equal, leads to simple expressions predicting that the phase of one mode advances whereas the phase of the other mode is retarded. When the yaw cards are uniformly spaced, the model leads to both growing and nongrowing yawing motion. Furthermore, a projectile traversing a uniformly spaced yaw card range can exhibit card-induced modal changes so that the measured overturning moment will be significantly different from the same measurement found in a nonintrusive spark range. These differences are most likely to be observed for small arm projectiles. Therefore, if a yaw card range is going to be used for extracting aerodynamic coefficients, one can consider the results given in this paper to help characterize and understand the yaw card induced disturbances.

References

[1] McCoy, R. L., "The Effect of Yaw Cards on the Pitching and Yawing Motion of Symmetric Projectiles," U.S. Army Ballistic Research Lab. Rept. BRL-TR-3338, Aberdeen Proving Ground, MD, May 1992 (AD 205633).

[2] Cooper, G. R., and Fansler. K. S., "Yaw Card Perturbaion of Projectile Dynamics," U.S. Army Research Lab. Rept. ARL-TR-1258, Aberdeen Proving Ground, MD, Jan. 1997.

[3] Murphy, C. H., "Free Flight Motion of Symmetric Missiles," U.S. Army Ballistic Research Lab., Rept. BRL-TR-1216, Aberdeen Proving Ground, MD, May 1963 (AD 442757).